Energy & Environmental Science

Cite this: *Energy Environ. Sci.*, 2011, **4**, 862

www.rsc.org/ees

COMMUNICATION

A facile preparation route for boron-doped graphene, and its CdTe solar cell application†

Tianquan Lin,[ab] Fuqiang Huang,*[ab] Jun Liang[a] and Yingxia Wang*[b]

Received 1st October 2010, Accepted 24th November 2010
DOI: 10.1039/c0ee00512f

High quality freestanding pristine graphene (PG) and boron-doped graphene (BG) were prepared by a novel and versatile method. BG is more conductive than PG due to a larger density of state generated near the Fermi level. Using BG as a back electrode, we achieved improved hole-collecting ability and photovoltaic efficiency for CdTe solar cells.

Graphene has recently attracted considerable attention owing to its excellent structural and electrical properties,[1] possible applications as a semiconductor, and applications as an excellent transparent conducting layer in dye-sensitized solar cells.[2,3] However, graphene is a zero-band-gap semiconductor with its density of states (DOS) at the Dirac point equal to zero, which is an obstacle for its use as a good conductor in electronics.[4,5] The Fermi level of graphene can be shifted, up or down, to increase the DOS by hole- or electron-doping, which has been predicted to modify the band structure. The work function of graphene has been calculated to be ~4.5 eV,[6] and the Fermi levels of 2 at.% (atom percent) boron- and nitrogen-doped graphene systems can be shifted by −0.65 and 0.59 eV, respectively.[7] As an electron-deficient dopant, boron can increase the work function of graphene, allowing it to serve as an ohmic back contact for CdTe solar cells, which until now have lacked a suitable metal for such function.

To date, two approaches have been developed to synthesize graphene. The top-down approach includes micromechanical,[8] thermal expansion,[9] chemical[10–12] or liquid-phase[13] exfoliation from bulk graphite, thermal decomposition of silicon carbide (SiC) substrate,[14] electrochemical synthesis,[15] and arc-discharge synthesis of multi-layered graphene.[16] The chemical exfoliation is a suitable method for mass production of graphene. However, graphene obtained by chemical exfoliation has very poor electrical conductivity owing to the structural defects formed during the vigorous exfoliation and reduction processes.[2] The bottom-up approach is based on chemical vapor deposition (CVD),[2,17] gas-phase synthesis assisted by microwave plasma[18] and solvothermal synthesis.[19] The presence of the substrate usually reduces the charge carrier mobility considerably because of the chemically bonded interface. Obviously, new synthetic methods are in demand for preparing graphene with the perfect hexagonal lattice to achieve excellent electrical transport properties.

In this study, we have explored a novel and versatile method to prepare freestanding pristine graphene (PG) and boron-doped graphene (BG). These graphenes form rapidly from nascent carbon and boron in the reduction reactions of tetrachloromethane (CCl_4) and boron tribromide (BBr_3) using an alkali metal (K) reductant. PG was

[a]*State Key Laboratory of High Performance Ceramics and Superfine Microstructure, Shanghai Institute of Ceramics, Chinese Academy of Sciences, Shanghai, 200050, P.R. China. E-mail: huangfq@mail.sic.ac.cn; Fax: +86 21 52416360; Tel: +86 21 52411620*
[b]*College of Chemistry and Molecular Engineering, Peking University, Beijing, 100871, P.R. China*

† Electronic supplementary information (ESI) available: Microscopic characterization of boron-doped graphene, flake thickness statistic, elemental abundances of products, FTIR spectrum analysis, synthesis of chemical reduced graphene, determination of the pristine graphene and boron-doped sizes, fabrication of film electrodes, and measurement and characterization. See DOI: 10.1039/c0ee00512f

Broader context

Graphene as a two-dimensional material has attracted considerable attention owing to its excellent electrical properties and possible applications in semiconductor devices and solar cells. However, synthesis of high-quality free-standing graphene and boron-doped graphene in large quantities remains a challenge. In this research, we have explored a novel and facile method to prepare free-standing graphene and boron-doped graphene, which were successfully incorporated as back contacts in CdTe solar cells for the first time. Thus prepared undoped graphene samples have fewer defects and better electrical transport performance than the exfoliated graphene oxide through chemical reduction with hydrazine hydrate. Similarly processed boron-doped graphene has a higher electrical conductivity and work function than pristine graphene due to a larger DOS generated near the Fermi level. Accordingly, our boron-doped graphene is able to improve the hole-collection ability and photovoltaic efficiency of CdTe solar cells, and, with a higher work function, it is a suitable metallic Ohmic back contact material which until now has been lacking for CdTe solar cells. We suggest that these materials would help to advance the research and applications of graphene and solar cells.

synthesized by reacting K (1.0 g) and CCl_4 (10.0 mL) in a sealed Teflon-lined stainless steel autoclave (50 mL). The autoclave was kept at 160 °C for 12 h, then cooled down to room temperature. The resultant product was dispersed in acetone under stirring to remove CCl_4 from the products. After filtering, the remaining product was washed with deionized water (1 L). The suspension was vacuum-filtered and dried in a vacuum oven at 100 °C for 12 h. BG was prepared following a similar procedure using CCl_4 (10 mL), K (1.2 g) and BBr_3 (52 μL), at 160 °C for 20 h. The yields of both PG and BG are approximately 0.4 g per 1 g of K.

The scanning electron microscope (SEM) and transmission electron microscope (TEM) images of the PG sample are displayed in Fig. 1. The architecture of the sheets and the nanostructured carbon products are clearly demonstrated. Before sonication, the sample consists of flower-like nanosheets, as shown in the SEM image (Fig. 1 (a)), and small stacked flakes, as shown in the TEM images (Fig. 1 (b)). In a number of cases we observed folded graphene layers (Fig. 1 (c)). In some cases the sheet edges tended to scroll and fold slightly. After sonication for 40 min in ethanol, single-layer graphene sheets with a topographic height of ~0.7 nm, consistent with that reported for single graphene,[10,20] were observed by atomic force microscopy (AFM), as shown in Fig. 1 (d). These results indicate that the present method can conveniently synthesize single-layer and few-layer graphene sheets. By analyzing a large number of TEM images, paying close attention to the uniformity of the flake edges, we estimated the percentage of single-layer graphene as 13.6% with flake-thickness statistics as shown in Figure S2 of the ESI†. The morphology of BG is the same as PG, as shown in Figure S1 of the ESI†. These graphene samples were used for further physical property measurements and device fabrication.

As shown in the X-ray photoemission spectroscopy (XPS) in Fig. 2 (a), the BG nanosheets have a binding energy peak (B-1s) at 191.5 eV while the C-1s peak is located at 284.8 eV (Fig. 2 (a) inset). The higher binding energy of BG, compared with that of pure boron (188 eV),

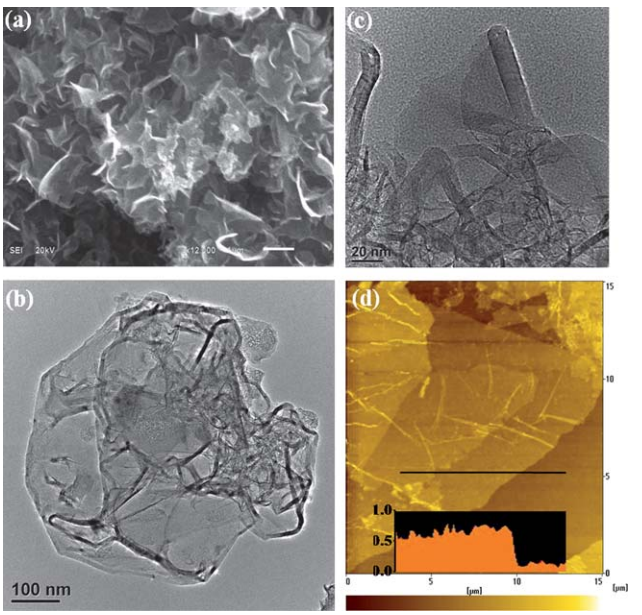

Fig. 1 (a) SEM, (b, c) TEM, and (d) AFM images of the pristine graphene sample. The scale bar in (a) is 1 μm.

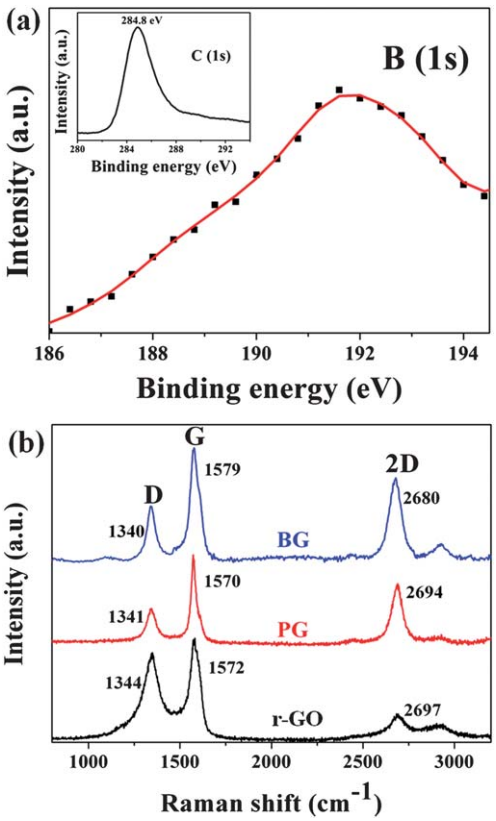

Fig. 2 (a) The B 1s and C 1s XPS spectra of boron-doped graphene (C 1s in the inset), (b) Raman spectra of pristine graphene (PG), boron-doped (BG), and chemically reduced exfoliated graphene oxide using hydrazine hydrate reductant (r-GO).

indicates that the boron atoms are bonded to carbon atoms in the sp^2 carbon network.[21] The content of boron was determined to be 1.1 at. % based on the XPS intensity measurement, listed in Table S1 of the ESI†. In the low-doping regime (~1 at. %), the band structure of BG is expected to be similar to the sp^2 carbon network of graphene. Oxygen traces, most likely from the adsorbed water according to the Fourier transform infrared spectroscopy (Figure S3†), were determined to be 7.22 at.% for PG and 7.66 at.% for BG using XPS.

Raman spectroscopy is a powerful nondestructive tool to determine the quality of graphene. In Fig. 2 (b), we compare Raman spectra of PG, BG, and a chemically reduced graphene oxide (r-GO, its preparation procedure using hydrazine hydrate as reductant is described in the ESI†). PG revealed the presence of the D (1341 cm^{-1}), G (1570 cm^{-1}), and 2D (2694 cm^{-1}) bands in Fig. 2 (b). Due to the selection rule, the D band, which is the breathing mode of the sp^2 rings, requires a defect for it to be activated. The G band results from first-order scattering of the E_{2g} mode of the sp^2 carbon domains. The 2D band is a second-order two-phonon mode. As shown in Fig. 2 (b), PG exhibits a sharp 2D peak located at 2694 cm^{-1}, while the r-GO exhibits a much broader set of split peaks around 2697 cm^{-1}. The intensity ratio of the G and D bands, I_G/I_D ~3, in PG is higher than that (I_G/I_D ~1) of r-GO, indicating that PG contains fewer defects than r-GO. The defects activating the D band may come from the edges and ripples in the nanosheets.[22] Comparing BG with PG, we find the I_G is much higher in BG and the ratio I_{2D}/I_G is smaller in BG. The decreased I_{2D}/I_G value may be attributed to BG's increased

absolute value of the Fermi level ($|E_F|$).[23] In addition to peak intensity, the shifts of the G-band frequencies can be interpreted in terms of the size of the C–C ring and the changes in the electronic structure.[24] The G band position (1579 cm^{-1}) in BG has a blue shift of 9 cm^{-1} over that of PG (1570 cm^{-1}). This is consistent with the higher electron concentration in BG: the frequency of the E_{2g} Γ phonon (Raman G band) increases with electron concentration due to the nonadiabatic removal of the Kohn anomaly at Γ-point.[25–27] In contrast, there is no obvious peak shift from PG to r-GO (1572 cm^{-1}). In addition, the 2D band is also sensitive to doping:[28] the 14 cm^{-1} red-shift of the BG 2D band relative to PG results from a decrease in the vibration frequency due to the increased lattice constant (which is due to the boron substitution).[29] The average sheet sizes for PG and BG, calucated from the Raman data,[30,31] are 56 and 35 nm, respectively. (See Equation S1 in the ESI† for the calculation.)

As discussed above, boron doping introduces more holes to the valence band of the graphene sheet, and a larger carrier concentration in the sample is achieved. To verify this, the electrical conductivities of r-GO, PG, and BG were compared using electrochemical impedance spectra (EIS). For these measurements, film electrodes, fabricated by a blade coating method described in ESI†, were obtained using r-GO, PG and BG. The Nyquist plots in Fig. 3 (a) show a smaller semicircle for PG than for r-GO, indicating a better conductivity for PG; the conductivity of BG is even higher. The improved conductivity cannot be attributed to the sheet size since the sheet size of most of the r-GO is between 5 μm and 20 μm according to Figure S4 of the ESI†, which is much larger than PG and BG. (The conductivity of graphene increases with the sheet size.) Therefore, BG and PG must have fewer defects than r-GO, which is consistent with the Raman spectra. The especially low impedance of the BG sample probably also reflects the increased DOS value near the Fermi level.

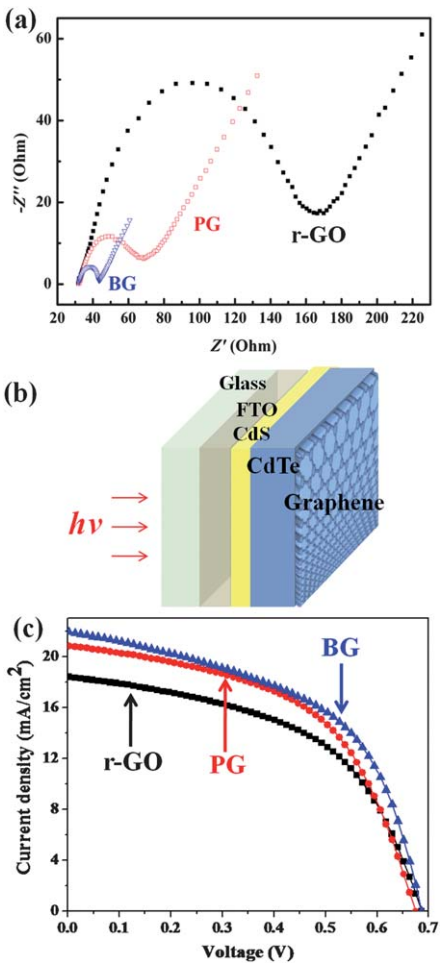

Fig. 3 (a) The typical electrochemical Nyquist plots of the r-GO-modified, PG-modified and BG-modified electrodes, (b) the schematic of the CdTe solar cell with a graphene back electrode, and (c) *I–V* characteristics of CdTe solar cells with different back electrodes.

Table 1 Photovoltaic performance of r-GO-, PG-, and BG-based CdTe solar cells

Back electrode	J_{sc}/mA cm^{-2}	V_{oc}/V	*FF* (%)	η (%)
r-GO	18.38	0.685	51.6	6.50
PG	20.81	0.674	52.9	7.41
BG	21.96	0.685	52.2	7.86

Conductive graphite paste is a good electrode (back contact) material to be used in CdTe solar cells. The work function of graphite nearly matches the CdTe absorber, and the highly polarized valence orbitals of Te (6s and 6p) have a rather intense chemical interaction with the delocalized C $3p_z$ orbitals. In a CdTe solar cell, the CdTe absorber generates holes, which are injected into the graphite electrode. Electrical conduction of graphite is anisotropic, and the hole conductivity (30–50 S cm^{-1}) perpendicular to the graphite layer is rather small compared with the in-plane conductivity (10^6 S cm^{-1}),[32] reflecting a weaker interaction between layers (van der Waals forces with a slightly delocalized π–π* interaction). Graphene only has in-plane conductivity, even multilayer graphene with a perfectly hexagonal carbon lattice is expected to have lower electrical conductivity along the *c* direction (perpendicular to the graphene layer) than normal graphite. Since BG has the lowest impedance, it is expected to act as a better back electrode for CdTe solar cells than PG, r-GO, or regular conductive carbon.

To demonstrate the suitability of PG and BG as back electrode materials for CdTe solar cells, solar cells shown in Fig. 3 (b) were fabricated. The current–voltage (*I–V*) curves of the devices are shown in Fig. 3 (c) and the measured photovoltaic parameters are listed in Table 1. For a 1.0 cm^2 CdTe solar cell with a PG-based back electrode, a short-circuit photocurrent density (J_{sc}) of 20.81 mA cm^{-2} with an open-circuit voltage (V_{oc}) of 0.674 V, a calculated fill factor (*FF*) of 52.9%, and an overall power conversion efficiency (η) of 7.41% have been obtained. The overall power conversion efficiency is considerably higher than that of the r-GO-based cell (6.50%), and it is also higher than a comparable cell using carbon nanotube arrays as a back electrode (7%).[33] As expected, the BG-based cell has an even higher efficiency (7.86%), indicating that the highly-conductive BG can improve the hole-collecting ability and reduce the barrier height to enhance the overall power conversion efficiency. The J_{sc} value of the BG-based cell, 21.96 mA cm^{-2}, is also higher than those of the r-GO and PG-based cells. The improved overall power conversion efficiency of the BG-based cell also reflects its higher work function helping to form an ohmic contact with the *p*-CdTe.

In summary, a new bottom-up technique was developed to prepare free-standing and high-quality pristine graphene and boron-doped graphene nanosheets. The as-prepared graphene samples were successfully applied to CdTe solar cells, used as back contacts, for the

first time. The as-prepared graphene with fewer defects has better electrical transport performance than the chemically reduced exfoliated graphene oxide sheets using hydrazine hydrate as reductant. The boron-doped graphene sample has an even better electrical conductivity and a higher work function than the pristine graphene due to a larger DOS generated near the Fermi level. Accordingly, the boron-doped graphene has a favorable effect on improving the hole-collection ability and the photovoltaic efficiency of CdTe solar cells. By adopting these graphenes as back electrodes, the photovoltaic efficiency of CdTe cells was increased from 6.50% for chemically (hydrazine hydrate) reduced graphene oxide to 7.41% for pristine graphene to 7.86% for boron-doped graphene.

Acknowledgements

The authors thank Prof. I-Wei Chen for his help. Financial support from National 973 Program of China Grant No. 2007CB936704 & 2009CB939903, NSF of China Grant No. 50772123 & 10775171, and Science and Technology Commission of Shanghai Grant No. 10520706700 & 0952nm06500 is acknowledged.

References

1 A. K. Geim and K. S. Novoselov, *Nat. Mater.*, 2007, **6**, 183.
2 K. S. Kim, Y. Zhao, H. Jang, S. Y. Lee, J. M. Kim, K. S. Kim, J. H. Ahn, P. Kim, J. Y. Choi and B. H. Hong, *Nature*, 2009, **457**, 706.
3 X. Wang, L. Zhi and K. Mullen, *Nano Lett.*, 2008, **8**, 323.
4 B. Uchoa and A. H. Castro Neto, *Phys. Rev. Lett.*, 2007, **98**, 146801.
5 X. R. Wang, X. L. Li, L. Zhang, Y. Yoon, P. K. Weber, H. L. Wang, J. Guo and H. J. Dai, *Science*, 2009, **324**, 768.
6 S. J. Sque, R. Jones and P. R. Briddon, *Phys. Status Solidi A*, 2007, **204**, 3078.
7 L. S. Panchokarla, K. S. Subrahmanyam, S. K. Saha, A. Govindaraj, H. R. Krishnamurthy, U. V. Waghmare and C. N. R. Rao, *Adv. Mater.*, 2009, **21**, 4726.
8 K. S. Novoselov, A. K. Geim, S. V. Morozov, D. Jiang, Y. Zhang, S. V. Dubonos, I. V. Grigorieva and A. A. Firsov, *Science*, 2004, **306**, 666.
9 M. J. McAllister, J. L. Li, D. H. Adamson, H. C. Schniepp, A. A. Abdala, J. Liu, M. Herrera-Alonso, D. L. Milius, R. Car, R. K. Prud'homme and I. A. Aksay, *Chem. Mater.*, 2007, **19**, 4396.
10 D. Li, M. B. Muller, S. Gilje, R. B. Kaner and G. G. Wallace, *Nat. Nanotechnol.*, 2008, **3**, 101.
11 G. X. Wang, J. Yang, J. Park, X. L. Gou, B. Wang, H. Liu and J. Yao, *J. Phys. Chem. C*, 2008, **112**, 8192.
12 S. Stankovich, D. A. Dikin, R. D. Piner, K. A. Kohlhaas, A. Kleinhammes, Y. Jia, Y. Wu, S. T. Nguyen and R. S. Ruoff, *Carbon*, 2007, **45**, 1558.
13 Y. Hernandez, V. Nicolosi, M. Lotya, F. M. Blighe, Z. Sun, S. De, I. T. McGovern, B. Holland, M. Byrne, Y. K. Gun'Ko, J. J. Boland, P. Niraj, G. Duesberg, S. Krishnamurthy, R. Goodhue, J. Hutchison, V. Scardaci, A. C. Ferrari and J. N. Coleman, *Nat. Nanotechnol.*, 2008, **3**, 563.
14 C. Berger, Z. M. Song, X. B. Li, X. S. Wu, N. Brown, C. Naud, D. Mayou, T. B. Li, J. Hass, A. N. Marchenkov, E. H. Conrad, P. N. First and W. A. de Heer, *Science*, 2006, **312**, 1191.
15 N. Liu, F. Luo, H. X. Wu, Y. H. Liu, C. Zhang and J. Chen, *Adv. Funct. Mater.*, 2008, **18**, 1518.
16 N. Li, Z. Wang, K. Zhao, Z. Shi, Z. Gu and S. Xu, *Carbon*, 2010, **48**, 255.
17 A. Reina, X. Jia, J. Ho, D. Nezich, H. Son, V. Bulovic, M. S. Dresselhaus and J. Kong, *Nano Lett.*, 2009, **9**, 30.
18 A. Dato, V. Radmilovic, Z. Lee, J. Phillips and M. Frenklach, *Nano Lett.*, 2008, **8**, 2012.
19 M. Choucair, P. Thordarson and J. A. Stride, *Nat. Nanotechnol.*, 2009, **4**, 30.
20 Z. S. Wu, S. F. Pei, W. C. Ren, D. M. Tang, L. B. Gao, B. L. Liu, F. Li, C. Liu and H. M. Cheng, *Adv. Mater.*, 2009, **21**, 1756.
21 L. S. Panchakarla, A. Govindaraj and C. N. R. Rao, *ACS Nano*, 2007, **1**, 494.
22 J. Campos-Delgado, J. M. Romo-Herrera, X. T. Jia, D. A. Cullen, H. Muramatsu, Y. A. Kim, T. Hayashi, Z. F. Ren, D. J. Smith, Y. Okuno, T. Ohba, H. Kanoh, K. Kaneko, M. Endo, H. Terrones, M. S. Dresselhaus and M. Terrones, *Nano Lett.*, 2008, **8**, 2773.
23 A. Das, S. Pisana, B. Chakraborty, S. Piscanec, S. K. Saha, U. V. Waghmare, K. S. Novoselov, H. R. Krishnamurthy, A. K. Geim, A. C. Ferrari and A. K. Sood, *Nat. Nanotechnol.*, 2008, **3**, 210.
24 Q. H. Yang, P. X. Hou, M. Unno, S. Yamauchi, R. Saito and T. Kyotani, *Nano Lett.*, 2005, **5**, 2465.
25 M. Lazzeri and F. Mauri, *Phys. Rev. Lett.*, 2006, **97**, 266407.
26 C. Casiraghi, *Phys. Rev. B: Condens. Matter Mater. Phys.*, 2009, **80**, 233407.
27 S. Pisana, M. Lazzeri, C. Casiraghi, K. S. Novoselov, A. K. Geim, A. C. Ferrari and F. Mauri, *Nat. Mater.*, 2007, **6**, 198.
28 W. Chen, S. Chen, D. C. Qi, X. Y. Gao and A. T. S. Wee, *J. Am. Chem. Soc.*, 2007, **129**, 10418.
29 L. S. Panchakarla, K. S. Subrahmanyam, S. K. Saha, A. Govindaraj, H. R. Krishnamurthy, U. V. Waghmare and C. N. R. Rao, *Adv. Mater.*, 2009, **21**, 4726.
30 K. Sato, R. Saito, Y. Oyama, J. Jiang, L. G. Cançado, M. A. Pimenta, A. Jorio, G. G. Samsonidze, G. Dresselhaus and M. S. Dresselhaus, *Chem. Phys. Lett.*, 2006, **427**, 117.
31 L. G. Cancado, K. Takai, T. Enoki, M. Endo, Y. A. Kim, H. Mizusaki, A. Jorio, L. N. Coelho, R. Magalhaes-Paniago and M. A. Pimenta, *Appl. Phys. Lett.*, 2006, **88**, 163106.
32 K. S. Krishnan and N. Ganguli, *Nature*, 1939, **144**, 667.
33 R. E. Camacho, A. R. Morgan, M. C. Flores, T. A. McLeod, V. S. Kumsomboone, B. J. Mordecai, R. Bhattacharjea, W. Tong, B. K. Wagner, J. D. Flicker, S. P. Turano and W. J. Ready, *JOM*, 2007, **59**, 39.